IEEE copyright notice

Derivation of the Frequency Mismatch Probability in Linear FMCW Radar based on Target Distribution

Marcus Reiher and Bin Yang

Chair of System Theory and Signal Processing, Universität Stuttgart

Pfaffenwaldring 47, 70550, Stuttgart, Germany

email: {marcus.reiher, bin.yang}@Lss.uni-stuttgart.de

Abstract—**In LFMCW (linear frequency modulated continuous wave) radar, there is a nonzero probability for mismatches to occur under certain conditions. This probability strongly depends on the modulation employed as well as on the distribution of targets in the radar's field of view, i.e. the application of the radar sensor. Hence to reduce mismatches in a given application, an effective approach is to carefully design the modulation used. Instead of utilizing extensive simulations, we derive the distribution of mismatches analytically, solely based on the modulation parameters and a given distribution of targets. Based on that mismatch distribution, an application-specific optimization of the modulation is feasible.**

Index Terms—**chirp radar, FMCW, mismatch mitigation, waveform design**

I. INTRODUCTION

It is well known that LFMCW radar may cause target mismatches under certain conditions. Such mismatches can arise in the frequency matching step of the signal processing chain and may lead to so called ghost targets, if the remaining processing steps (e.g. tracking) are not able to identify them as mismatches. Most applications employing such a radar, however, are required to be robust with respect to ghost targets and hence mismatches. Especially in the field of automotive radar, there is an ongoing extension of radar applications from driver assistance systems, e.g. ACC (adaptive cruise control), to safety systems. Clearly, those systems do have an increasing demand for highly reliable sensor decisions and thus the avoidance of mismatches plays a major role in the design of an LFMCW radar system.

As the probability of mismatches depends on the radar signal modulation and the targets in the sensor's field of view, a good approach to reduce mismatch occurrence is to carefully design the modulation used. In order to accurately estimate the probability of mismatches in a given application, extensive simulations based on target statistics are commonly necessary. They search for an optimal modulation exhaustively and are computationally demanding.

In this paper, we show how to analytically derive the probability of mismatches at an arbitrary position of the so called distance-velocity-plane, based on a given distribution of targets and for an arbitrary modulation. The outline of this paper is as follows: In section II, we briefly review the basic properties and equations of the LFMCW radar. In section III, we derive the mismatch probability and give some extensions in section IV. Simulation results for various target distributions and modulations are presented in section V. Final conclusions are drawn in section VI.

II. LFMCW MODULATION

A. The LFMCW equation

We will not derive the basic equations of LFMCW here, as there are many excellent books about this topic like [1]. The most important equation is the so called LFMCW equation, linking the target parameters to be estimated, distance d[m]

and relative radial velocity (negative for closing targets) $v[\frac{m}{s}]$, to the beat frequency f[Hz], defined as the difference between the transmitted and the received frequency. The radar's transmit frequency is swept linearly as a function of time, with a slope of $s[\frac{Hz}{s}]$ and centered at the carrier frequency f_c[Hz]. We call such an up- or downsweep a frequency ramp, or simply a ramp. The resulting beat frequency f is then given by

$$f = \frac{2}{c}(sd + f_c v) = \underbrace{\frac{2}{c} \begin{bmatrix} s & f_c \end{bmatrix}}_{\underline{a}^T} \underbrace{\begin{bmatrix} d \\ v \end{bmatrix}}_{\underline{p}} = \underline{a}^T \underline{p}, \quad (1)$$

where c is the speed of light. Equation (1) corresponds to a straight line in the (dv)-plane

$$v = -\frac{s}{f_c}d + \frac{cf}{2f_c}, \quad (2)$$

a so called (dv)-line. For an up- (positive slope) or downsweep (negative slope) of the transmit frequency, the (dv)-line decays or rises linearly. To determine the unknown target parameters (d, v), a second ramp with a different slope is necessary. The target is then located at the intersection of both (dv)-lines. In general, when we use N ramps to measure M targets, the target parameters are determined at the intersection of all (dv)-lines. Approximate intersections have to be accounted for, too, due to measuring errors in practice. The method to perform the aforementioned search for intersections is called frequency matching, refer to [2] or [3] for a brief introduction.

B. Frequency matching

No matter how many ramps are used in a modulation, it is always possible to construct a pattern of $M(\geq N)$ targets that causes more than M intersections of N (dv)-lines. The result is the occurrence of mismatches, refer to Fig. 1. This means, N ramps are not always enough to determine $M(\geq N)$ targets uniquely, but there will be no mismatches if $M < N$.
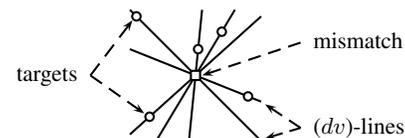
Fig. 1.   A mismatch for $M \geq N$ targets, here $N = M = 5$

It is reasonable to conjecture that, the more ramps we use in a modulation, the smaller the probability of mismatches is. Yet, to our knowledge, there have only been few attempts to study theoretically the impact of the design of a modulation to mismatches. The optimal modulation from both points of view, target detection and target parameter estimation, has been derived in [4] utilizing the concept of mutual information. In [2], formulas for

the mean number of mismatches for modulations with three or four ramps are given, based on a uniform distribution of the beat frequency. Upper bounds for the number of mismatches are given in [5]. To optimize a modulation for a specific application, however, it is desirable to know the distribution of mismatches as accurate as possible.

III. DERIVATION OF THE MISMATCH PROBABILITY

A. Preparatory remarks

In this section, we derive the probability of mismatch which occurs at an arbitrary position of the (dv)-plane, based on a given modulation and distribution of targets. First we introduce some definitions:

- The a priori probability density function (pdf) for the occurrence of a target at a specific position of the (dv)-plane is modeled by the bivariate density function of the continuous random variables distance D and relative radial velocity V:

$$p_{dv} := \frac{\partial^2}{\partial d \partial v} P(D \le d, V \le v) \qquad (3)$$

Throughout the paper, $P(X)$ is used to denote the probability for the occurrence of event X and $P(X,Y) := P(X \cap Y)$. We partition the (dv)-plane into (not necessarily) rectangular cells ζ of size Δd and Δv and the probability for a target to occur inside the cell ζ_0 centered at (d_0, v_0) is

$$P_{d_0 v_0} = p_{d_0 v_0} \Delta d \Delta v, \qquad (4)$$

refer to Fig. 2. p_{dv} can either be estimated from real measurements or modeled based on some a priori knowledge of the target distribution.
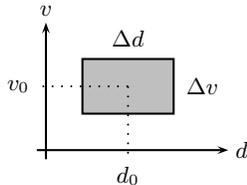
Fig. 2. (dv)-cell ζ_0 at (d_0, v_0)

- According to (1), the N-ramp modulation is described by

$$\mathbf{A} := \begin{bmatrix} \underline{a}_1^T \\ \vdots \\ \underline{a}_N^T \end{bmatrix} = \frac{2}{c} \begin{bmatrix} s_1 & f_c \\ \vdots & \vdots \\ s_N & f_c \end{bmatrix}. \qquad (5)$$

In addition, we define the following events for an arbitrary (dv)-cell ζ_0 at (d_0, v_0):

- T: A target resides in ζ_0.
- S: An intersection of (dv)-lines is detected in ζ_0.
- F: A mismatch occurs in ζ_0.

A mismatch occurs in ζ_0 if all N (dv)-lines of different slopes intersect inside ζ_0 but no target resides there, refer to Fig. 1. If multiple targets reside inside the same (dv)-cell, they are treated as a single target in this paper, since a separation could only be achieved by other methods like angle estimation which is not considered here.

With these definitions, the frequency matching of the LFMCW radar can be viewed as a binary erroneous channel, with the mismatch illustrated by the bold line in Fig. 3. Obviously, the
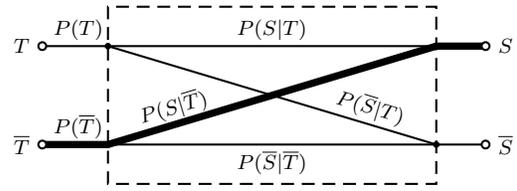
Fig. 3.   Frequency matching as a binary erroneous channel

probability for the occurrence of a mismatch in ζ_0 can be expressed as

$$P(F) = P(\overline{T}, S) = P(\overline{T})P(S|\overline{T}) =: P_{\text{FA}}(\zeta_0). \qquad (6)$$

$\overline{X}$ denotes the complementary event of X and $P(X|Y)$ is the probability of X conditioned on Y.

B. Base formula

In this section, we derive the base formula expressing the probability of mismatch in an arbitrary cell ζ_0 as a function of both the modulation and target distribution. We aim to derive $P_{\text{FA}}(\zeta_0)$ as a function of the modulation $\mathbf{A}$, target pdf p_{dv} and detection properties $P_{\text{D},i}$ and $P_{\text{FA},i}$ with

- $P_{\text{D},i}$: Probability of spectral detection in ramp i, i.e. the probability that a truly existing target beat frequency is detected in the spectrum of ramp i.
- $P_{\text{FA},i}$: Probability of spectral false alarm in ramp i, i.e. the probability that a truly *not* existing target beat frequency is detected in the spectrum of ramp i.

For this purpose, we need two new events for ramp i:

- T_i: A beat frequency *exists* in the spectrum of ramp i whose corresponding (dv)-line passes the ζ_0 cell.
- S_i: A beat frequency is *detected* in the spectrum of ramp i whose corresponding (dv)-line passes the ζ_0 cell.

Under the assumption that only intersections of all N (dv)-lines are regarded as a target (an extension for lower intersection orders is given in section IV-B), we have

$$S = \bigcap_{i=1}^{N} S_i \quad \text{with} \quad P(S) \neq \prod_{i=1}^{N} P(S_i), \qquad (7)$$

as the events S_i and S_j are not independent in general. This is, for example, the case if a target resides in cell ζ_0. Independence is guaranteed only if the event $\overline{T}$ is true and all spectral false alarm detections are independent. Then we have

$$P(S|\overline{T}) = P\left(\left(\bigcap_{i=1}^{N} S_i \right) |\overline{T} \right) = \prod_{i=1}^{N} P(S_i|\overline{T}). \qquad (8)$$

Additionally, $T \subset \bigcap_{i=1}^{N} T_i$ as shown in Fig. 1. This means, the presence of N different (dv)-lines passing the same ζ_0-cell does not necessarily imply that a target resides inside that cell. It follows

$$\overline{T} \supset \overline{\bigcap_{i=1}^{N} T_i} = \bigcup_{i=1}^{N} \overline{T_i} \supset \overline{T_i} \quad \text{and} \quad \overline{T_i} \cap \overline{T} = \overline{T_i} \quad \forall i. \qquad (9)$$

Now we introduce a new discrete random variable

- K_i: Number of targets whose (dv)-lines pass the ζ_0-cell in ramp i.

We also define a quantized (dv)-line in the (dv)-plane as

$$R_i := \{\zeta \mid \zeta \text{ passed by the } (dv)\text{-line of ramp } i \text{ through } \zeta_0\}$$

$$= \{(d,v) \mid v \approx -\frac{s_i}{f_c} d + (v_0 + \frac{s_i}{f_c} d_0)\}, \qquad (10)$$
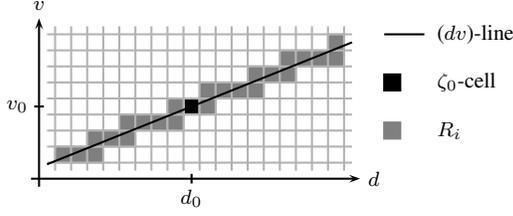
Fig. 4. Sketch of quantized (dv)-line R_i

see Fig. 4. The actual calculation of R_i is simpler and differs slightly from the illustration in Fig. 4: All (dv)-cells are regarded as part of the quantized (dv)-line R_i, whose frequencies differ from the center frequency of cell ζ_0 less than a fixed amount Δf_i. In our implementation, Δf_i was chosen to be $\Delta f_i = 1.2/\tau_i$ [FFT bin/s], where τ_i is the duration of ramp i. This means, two beat frequencies in spectrum i with a frequency difference larger than Δf_i cannot contribute to the same (dv)-line. Following (8), we continue with

$$P(S_i|\overline{T}) = \frac{P(S_i, \overline{T})}{P(\overline{T})} = \frac{P(S_i, \overline{T_i}, \overline{T}) + P(S_i, T_i, \overline{T})}{P(\overline{T})} \quad (11)$$

and consider that

$$P(\overline{T}) = 1 - P_{\zeta_0} = 1 - P_{d_0 v_0}, \quad (12)$$
$$P(\overline{T_i}) = P(K_i = 0) = \prod_{\zeta \in R_i} (1 - P_\zeta). \quad (13)$$

Equation (13) follows from the fact that the events T_i and $K_i > 0$ are equivalent. It follows

$$\frac{P(S_i, \overline{T_i}, \overline{T})}{P(\overline{T})} \overset{(9)}{=} \frac{P(S_i, \overline{T_i})}{P(\overline{T})} = \underbrace{P(S_i|\overline{T_i})}_{P_{\mathrm{FA},i}} \frac{P(\overline{T_i})}{P(\overline{T})}$$

$$\overset{(12),(13)}{=} P_{\mathrm{FA},i} \prod_{\zeta \in R_i \setminus \zeta_0} (1 - P_\zeta), \quad (14)$$

$$\frac{P(S_i, T_i, \overline{T})}{P(\overline{T})} = \frac{1}{P(\overline{T})} \sum_{k=1}^{\infty} P(S_i, K_i = k, \overline{T})$$

$$= \sum_{k=1}^{\infty} P(S_i|K_i = k, \overline{T}) P(K_i = k|\overline{T}). \quad (15)$$

We realize that the first term in (15) can be rewritten as

$$P(S_i|K_i = k, \overline{T}) = 1 - P(\overline{S_i}|K_i = k, \overline{T})$$
$$= 1 - (1 - P_{\mathrm{D},i})^k, \quad (16)$$

if we assume that the miss detections of the $K_i = k$ beat frequencies are independent. With the approximation

$$P(K_i > 1) \approx 0, \quad (17)$$

we finally obtain

$$\frac{P(S_i, T_i, \overline{T})}{P(\overline{T})} \overset{(16)}{=} \sum_{k=1}^{\infty} \left(1 - (1 - P_{\mathrm{D},i})^k\right) P(K_i = k|\overline{T})$$

$$\overset{(17)}{\approx} P_{\mathrm{D},i} P(K_i = 1|\overline{T})$$

$$= P_{\mathrm{D},i} \sum_{\zeta_1 \in R_i \setminus \zeta_0} P_{\zeta_1} \prod_{\zeta_2 \in R_i \setminus \{\zeta_0, \zeta_1\}} (1 - P_{\zeta_2})$$

$$= P_{\mathrm{D},i} \sum_{\zeta_1 \in R_i \setminus \zeta_0} \frac{P_{\zeta_1}}{1 - P_{\zeta_1}} \frac{P(\overline{T_i})}{P(\overline{T})}. \quad (18)$$

If necessary, Eq. (18) can be further improved by taking additional terms with $K_i \geq 2$ into account.

With this, all parts needed to compute $P_{\mathrm{FA}}(\zeta_0)$ have been derived:

$$P_{\mathrm{FA}}(\zeta_0) \overset{(6)}{=} P(\overline{T})P(S|\overline{T}) \overset{(8)}{=} P(\overline{T}) \prod_{i=1}^{N} P(S_i|\overline{T})$$

$$\overset{(11),(14),(18)}{\approx} P(\overline{T}) \prod_{i=1}^{N} \frac{P(\overline{T_i})}{P(\overline{T})}$$

$$\cdot \left(P_{\mathrm{FA},i} + P_{\mathrm{D},i} \sum_{\zeta \in R_i \setminus \zeta_0} \frac{P_\zeta}{1 - P_\zeta} \right)$$

$$\overset{(12),(13)}{=} (1 - P_{\zeta_0}) \prod_{i=1}^{N} \left(\prod_{\zeta \in R_i \setminus \zeta_0} (1 - P_\zeta) \right)$$

$$\cdot \left(P_{\mathrm{FA},i} + P_{\mathrm{D},i} \sum_{\zeta \in R_i \setminus \zeta_0} \frac{P_\zeta}{1 - P_\zeta} \right). \quad (19)$$

First observations about the base formula (19) are:

- The larger the number of ramps N is, the lower the value of $P_{\mathrm{FA}}(\zeta_0)$ will be.
- The larger the false alarm probability $P_{\mathrm{FA},i}$ is, the larger the value of $P_{\mathrm{FA}}(\zeta_0)$ will be. The same also applies to $P_{\mathrm{D},i}$. The reason is that an increased number of detected (dv)-lines makes a mismatch more probable.
- A large value of $P_{\mathrm{FA}}(\zeta_0)$ is attained for such (dv)-cells, where all N quantized (dv)-lines R_i pass through regions of the target pdf that have a high probability for target occurrence.
- Under the assumption $P_{\mathrm{FA},i} = 0 \ \forall \ i$, a zero mismatch probability can be achieved for those cells, where it is possible to design at least one ramp which corresponding quantized (dv)-line has no intersection with the support of the target pdf. This will become more evident in section V.

IV. EXTENSIONS

In this section, we derive three useful extensions of the base formula (19).

A. Missing IQ-mixer

If the radar under consideration does not use an IQ-mixer, minor adaptations have to be applied to the base formula. Without IQ-mixer, the sign of a beat frequency is unknown, forcing us to take its negative value into account as well in the frequency matching. This leads to an adapted definition of a (dv)-line passing the ζ_0-cell. Without IQ-mixer, the single (dv)-line in (10) becomes two parallel (dv)-lines as illustrated in Fig. 5. Thus the event T_i can now be caused by (dv)-cells on either (dv)-lines with the beat frequency $\pm f$.

Obviously, $P_{\mathrm{FA}}(\zeta_0)$ is increased as there are more cells that cause
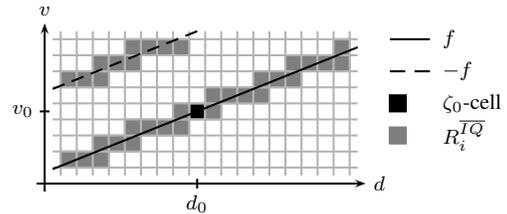
Fig. 5. Sketch of quantized (dv)-line R_i for missing IQ-mixer

the same absolute value of beat frequency as ζ_0. Formally, the quantized (dv)-line R_i passing the ζ_0-cell has to be changed to

$$R_i^{IQ} \rightarrow R_i^{\overline{IQ}} = \left\{ (d,v) \mid v \approx -\frac{s_i}{f_c}d \pm \left(v_0 + \frac{s_i}{f_c}d_0\right) \right\}, \quad (20)$$

in comparison to (10). No other changes are necessary in (19).

B. Arbitrary intersection order

In a real radar system there is no ideal detection, i.e. $P_{D,i} < 1$ and $P_{FA,i} > 0$. The probability of successful detection of all N frequencies of a real target is $\prod_{i=1}^{N} P_{D,i}$, if we assume the probability of detection in different spectra to be independent. If $P_{D,i}$ is significantly smaller than one, the overall probability of detection degrades noticeably. For a modulation with $N = 4$ ramps and $P_{D,i} = 0.9$, for example, all four beat frequencies of a real target will be detected in roughly two out of three cycles only. The value of $P_{D,i}$ can be increased, of course, but only at the cost of an increased false alarm probability $P_{FA,i}$. Thus intersections of a smaller number of (dv)-lines than N should be considered as valid targets as well. We call this number the *intersection order*.

Below we extend the base formula (19) to account for a minimum intersection order $N_{\min}$ ($2 \leq N_{\min} \leq N$). This introduces some changes in (7) and (8), where the single events S_i are combined to form the desired event S. For an exemplary modulation with $N = 3$ ramps and a minimum intersection order of $N_{\min} = 2$, the event S for detection of an intersection becomes

$$S = S_1 S_2 S_3 \cup \overline{S_1} S_2 S_3 \cup S_1 \overline{S_2} S_3 \cup S_1 S_2 \overline{S_3}$$

and thus

$$\begin{aligned} P(S) = & P(S_1 S_2 S_3) \\ & + P(\overline{S_1} S_2 S_3) + P(S_1 \overline{S_2} S_3) + P(S_1 S_2 \overline{S_3}). \end{aligned}$$

Hence Eq. (8) is changed to

$$\begin{aligned} P(S|\overline{T}) = & \sum_{q=N_{\min}}^{N} \left\{ \sum_{\Psi = \{1,\ldots,N\}_q} \left[\left(\prod_{i \in \Psi} P(S_i|\overline{T}) \right) \right.\right. \\ & \left.\left. \cdot \left(\prod_{j \in \{1,\ldots,N\}\setminus\Psi} P(\overline{S}_j|\overline{T}) \right) \right] \right\}, \quad (21) \end{aligned}$$

where we used $\Psi = \{1,\ldots,N\}_q$ as a shortcut for any subset of $\{1,\ldots,N\}$ with q elements.

C. Varying frequency detection performance

In the base formula (19), both $P_{D,i}$ and $P_{FA,i}$ are assumed to be constant. A more realistic approach is to model both $P_{D,i}$ and $P_{FA,i}$ as a function of various sensor and signal parameters like

- Frequency detection algorithm.
- Signal-to-noise ratio (SNR), in particular varying SNR over frequency due to street clutter.
- Automatic gain control (AGC) of the sensor amplifier.
- Power leakage from Tx to Rx.

This will be done in the future.

V. SIMULATION RESULTS

To give an impression about the mismatch probability, simulations have been carried out for different target pdfs using the base formula (19) and it's extensions. All target distributions are defined for $0\text{m} \leq d \leq 250\text{m}$ and $-60\frac{\text{m}}{\text{s}} \leq v \leq 30\frac{\text{m}}{\text{s}}$ and quantized in rectangular cells of size $\Delta d = 0.25\text{m}$ and $\Delta v = 0.25\frac{\text{m}}{\text{s}}$.

modulation	ramp	slope [MHz/ms]	duration [ms]
A	1,2	± 150.0	1.00
	3,4	± 3.0	7.50
B	1,2	± 150.0	1.00
	3,4	± 75.0	2.00
C	1,2	± 150.0	1.00
	3	75.0	2.00
D	1,2	± 150.0	1.00
	3,4	± 75.0	2.00
	5	3.0	7.50

TABLE I
PARAMETERS OF MODULATIONS A, B, C AND D

A. Modulation parameters

Four different modulations are used. Their parameters are given in Table I. All ramps are centered at $f_c = 76.5\text{GHz}$. A FFT of length 512 is applied to generate the spectra. The part of the (dv)-plane that can be sensed with the respective modulation is depicted in Fig. 6 for modulation A and B. Each plot shows the field of view as the non-hatched region of the (dv)-plane. For each modulation, there are as many hatched regions as the number of ramps (in Fig. 6(a), one of the hatched regions is very small and another one is totally outside the considered rectangular (dv)-plane. Each hatched region at the right-hand side is bounded by a (dv)-line of one frequency ramp for either $f = f_{\max}$ or $f = f_{\min}$, depending on the sign of the slope s. The lines for $f = 0\text{Hz}$ are shown at the left-hand side. Note that a rising frequency ramp (positive slope) corresponds to a falling (dv)-line according to (2) and vice versa. Both modulation A and B consist of four ramps where the first two ramps are identical. Modulation C consists of three ramps and is derived from modulation B by dropping the fourth ramp. Modulation D consists of five ramps and is derived from modulation B by adding the third ramp of modulation A.

(a) Modulation A
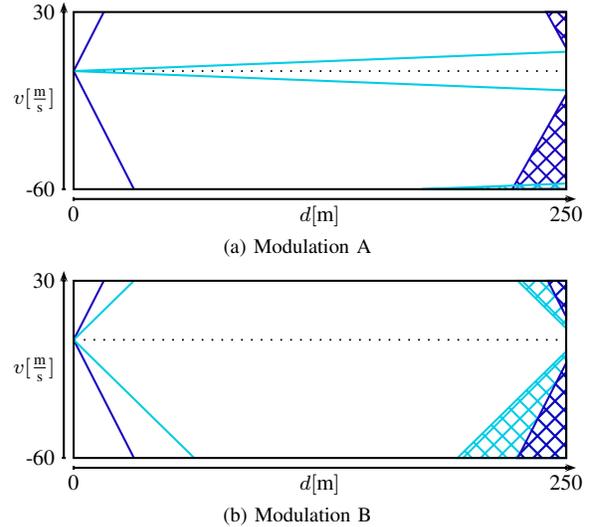
(b) Modulation B

Fig. 6.   Field of view of modulations A and B

B. Experiment 1: Ideal case

In the first experiment, the target distribution is assumed to be constant, i.e. targets are uniformly distributed in the considered rectangular (dv)-plane in Fig. 6. In addition, we use the following ideal settings:

(a) Modulation A
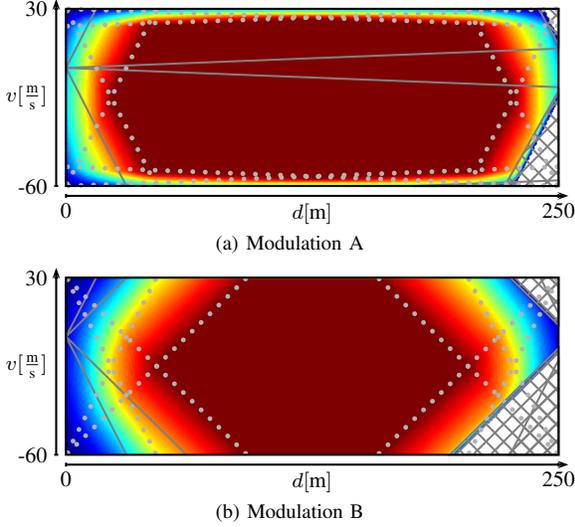
(b) Modulation B

Fig. 7. Mismatch probability of experiment 1

- $P_{D,i} = 1$ and $P_{FA,i} = 0 \ \forall \ i$
- IQ-mixer present
- Intersection order $N_{min} = N$.

Fig. 7 shows the calculated probabilities of mismatch for modulation A and B, overlayed with the field of view of each modulation. Each plot uses an individual linear color scale from blue to dark red to represent an increasing mismatch probability. The color white is reserved to show a zero mismatch probability. The hatched part of the (dv)-plane is white in this case since it is not observable by all N ramps due to $N_{min} = N$. For a quantitative comparison, Table II contains the numerical values of the maximum and average mismatch probability over all observable (dv)-cells of this experiment (and five additional ones reported later). We make the following observations:

- $P_{FA}(\zeta_0) > 0$ in the observable (dv)-plane, as the support of the target pdf covers the whole (dv)-plane.
- The maximum and average mismatch probability of modulation A and B are of the same order. Modulation C with three ramps achieves a higher and modulation D with five ramps attains a lower value of $P_{FA}(\zeta_0)$. This supports the statement in section III-B that adding further ramps decreases the mismatch probability of a modulation.
- For a uniform distribution of targets, the region with the highest $P_{FA}(\zeta_0)$ is bounded by those (dv)-lines that are caused by targets located at the four corners of the rectangular (dv)-plane. This is illustrated by the dotted lines in Fig. 7(a) and 7(b). Note that for each corner only two (dv)-lines are visible. The reason is that the factor $P(S_i|\overline{T})$ from Eq. (8) remains constant inside these bounds, as the number of (dv)-cells on the quantized (dv)-line R_i remains unchanged.

C. Experiment 2: Nonideal frequency detection

The second experiment uses the same simulation conditions as in experiment 1, i.e. uniform target pdf, IQ-mixer, $N_{min} = N$, except for a nonideal frequency detection with $P_{D,i} = 0.8$ and $P_{FA,i} = 10^{-3} \ \forall \ i$. As the overall appearance of $P_{FA}(\zeta_0)$ does not change much in comparison to Fig. 7, we only inspect the numerical values of $P_{FA}(\zeta_0)$ in Table II. Note that these values are normalized to those of experiment 1. We recognize

experiment	normalized to	modulation			
		A	B	C	D
maximum $P_{FA}(\zeta_0)$					
1	10^{-2}	0.13	0.22	1.00	0.04
2	exp. 1	0.43	0.41	0.52	0.34
3	exp. 1	3.23	1.45	1.47	2.35
4	exp. 1	18.54	15.32	11.96	20.43
5	10^{-2}	0.62	0.21	0.99	0.08
6	exp. 5	1.00	1.05	1.03	1.00
average $P_{FA}(\zeta_0)$					
1	10^{-4}	0.69	1.00	5.28	0.17
2	exp. 1	0.44	0.42	0.51	0.33
3	exp. 1	2.24	1.19	1.16	1.67
4	exp. 1	19.00	16.83	12.58	21.00
5	10^{-4}	0.14	0.31	1.92	0.02
6	exp. 5	1.24	1.18	1.13	1.82

TABLE II
MAXIMUM AND AVERAGE MISMATCH PROBABILITY

that both the maximum and average value of $P_{FA}(\zeta_0)$ are reduced to roughly 42% of experiment 1 for modulation A and B as well as 52% and 34% for modulation C and D, respectively. This is mainly due to the term $P_{D,i}^{N_{min}} \approx 0.41, 0.51, 0.33$ in Eq. (19) for $P_{D,i} = 0.8$ and $N_{min} = 4, 3, 5$ for modulation A/B, C, D. Hence, a lower frequency detection probability reduces the mismatch probability due to a reduced number of detected (dv)-lines.

D. Experiment 3: Missing IQ-mixer

The third experiment is identical to the first one except for a missing IQ-mixer. In this case, we have to use the extension of the base formula in Eq. (20). Fig. 8 shows the results of

(a) Modulation A
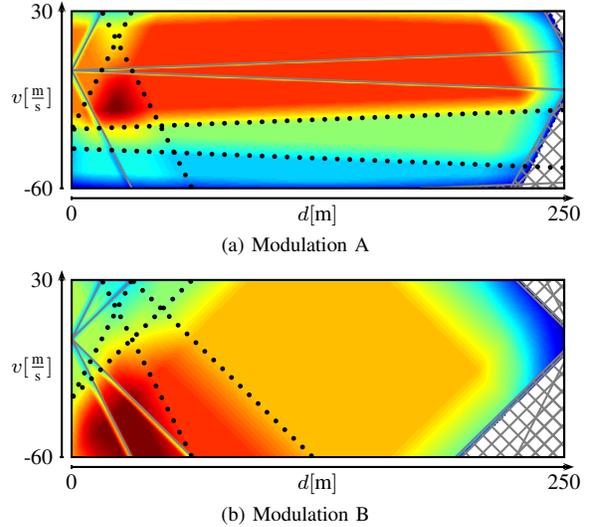
(b) Modulation B

Fig. 8. Mismatch probability of experiment 3

this experiment. As expected, Table II indicates an increased mismatch probability. The increase is larger for those modulations that exploit the benefits of an IQ-mixer more efficiently, i.e. modulations with shallow ramps (small $|s|$) such as modulation A and partly D. Additionally, we observe the following phenomena:

- The modulation design has a stronger influence on mismatch probability for a missing IQ-mixer.

- If an IQ-mixer is missing, $P_{\text{FA}}(\zeta_0)$ is considerably raised in those regions, where both f and $-f$ are observable. We already gave the reason in section IV-A, namely that two parallel (dv)-lines have to be accounted for in this case. These regions are located symmetrically around the (dv)-lines with $f = 0\text{Hz}$. Their borders are illustrated by the dotted lines in Fig. 8(a) and 8(b).

E. Experiment 4: Lower intersection order

The fourth experiment investigates the effect of a lower intersection order with $N_{\min} = N - 1$. The other simulation conditions are identical to experiment 1. The plots of $P_{\text{FA}}(\zeta_0)$ in the (dv)-plane are not shown here since they look similar to those in Fig. 7. One noticeable difference is that areas hatched only once in Fig. 6 become now visible, since a target detection requires now an intersection of $N - 1$ (dv)-lines only. Table II shows a large increase of $P_{\text{FA}}(\zeta_0)$ as predicted by (21). Interestingly, though the modulation C now allows for matches of two ramps, the values did not increase as much as for the other modulations. The reason is that if the number of ramps N decreases, the number of different submodulations decreases, too. With the present setting of $N_{\min} = N - 1$, there are N submodulations that add to the overall value of $P_{\text{FA}}(\zeta_0)$, refer to Eq. (21). Hence, for an intersection order of $N_{\min} < N$, the relative increase of $P_{\text{FA}}(\zeta_0)$ rises with the number of ramps of a modulation. Other observations are:

- A moderate increase in detection performance of real targets (roughly P_{D}^{N-1} versus P_{D}^{N}) induces a large increase in mismatch probability.
- The level of increase of mismatch probability varies for different modulations. Hence it seems fruitful to also optimize the submodulations, i.e. the N submodulations containing $N - 1$ ramps each.

F. Experiment 5 and 6: ACC target distribution

In experiment 5, we use the same ideal settings as in experiment 1 and a target pdf that is typical for the ACC application on highways. The target pdf is plotted in Fig. 9 and consists of two modes, one for stationary targets (ST) at the mean negative velocity of the ego vehicle ($v_{\text{ST}} \approx -25.2\frac{\text{m}}{\text{s}}$) and one for moving targets (MT) at $v_{\text{MT}} \approx 0\frac{\text{m}}{\text{s}}$. The distribution is explained in more detail in [3]. Fig. 10 shows the computed mismatch probability. Obviously, this distribution is more sensitive to modulation design than the uniform target pdf. Table II shows that modulation B has a smaller maximum probability, yet a much larger mismatch probability on average than modulation A.

In the final experiment 6, the ACC target pdf is combined with a missing IQ-mixer. Table II shows a moderate increase of $P_{\text{FA}}(\zeta_0)$ in comparison to experiment 5. Our conclusions are:
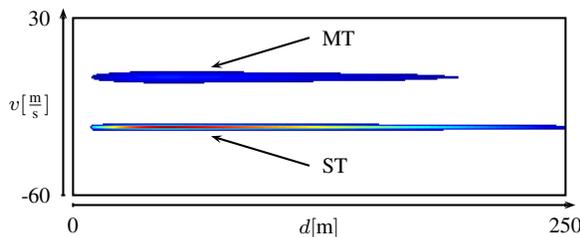
Fig. 9.   Target distribution for ACC scenarios

(a) Modulation A
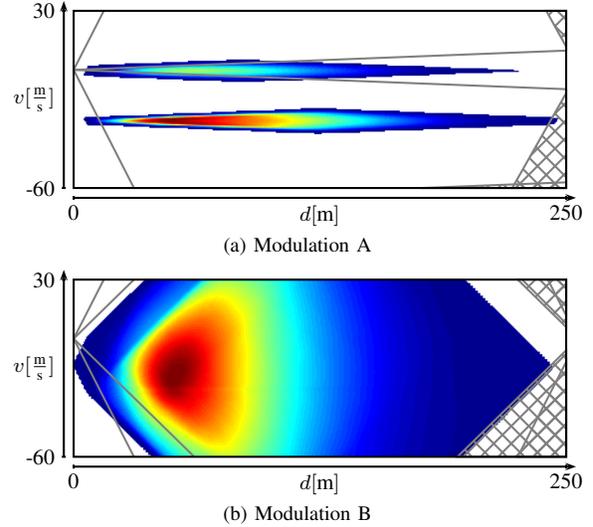
(b) Modulation B

Fig. 10.   Mismatch probability of experiment 5

- With the modulation adapted to the target pdf, a mismatch probability of zero can be achieved for a large part of the (dv)-plane, refer to Fig. 10(a).
- A disadvantage in Fig. 10(a) is, however, that all mismatches happen in the vicinity of the real targets. This makes the detection of isolated mismatches during the subsequent tracking more difficult. By taking tracking and isolated mismatches into account, modulation B is the better choice in comparison to modulation A.

VI. CONCLUSION

In this paper, we have derived a closed-form base formula for the mismatch probability in LFMCW radar based on a given target distribution and modulation parameters. We have also developed various extensions to the base formula to account for many nonidealities in the modulation design in practice. We presented and compared simulation results for various parameters, settings and demonstrated the usefulness of our formulas. The framework seems very promising to ease the optimization of LFMCW modulation with respect to the mismatch probability, what we will further investigate in future work.

REFERENCES

[1] N. Levanon and E. Mozeson, *Radar Signals*, 1st ed. Hoboken, New Jersey: John Wiley & Sons, 2004.
[2] M. Meinecke, "Zum optimierten Sendesignalentwurf fuer Automobilradare," Ph.D. dissertation, Technische Universitaet Hamburg-Harburg, 2001.
[3] M. Reiher and B. Yang, "Extending the Frequency Matching in Linear FMCW Radar Exploiting Extreme Frequencies," in *IEEE Radar Conference*, Pasadena, USA, May 2009.
[4] M. R. Bell, "Information Theory and Radar: Mutual Information and the Design and Analysis of Radar Waveforms and Systems," Ph.D. dissertation, California Institute of Technology, Pasadena, USA, Mar. 1988.
[5] M. Reiher and B. Yang, "On the Occurrence of Ghost Targets in Linear FMCW Radar: A Worst Case Study," in *International Radar Symposium*, Wroclaw, Poland, May 2008, pp. 31–34.